

Stochastic Signal Processing Methods for Shear Wave Imaging using Ultrasound



Atul Ingle
advised by Prof. Tomy Varghese

(Supported by NIH-NCI R01CA112192)

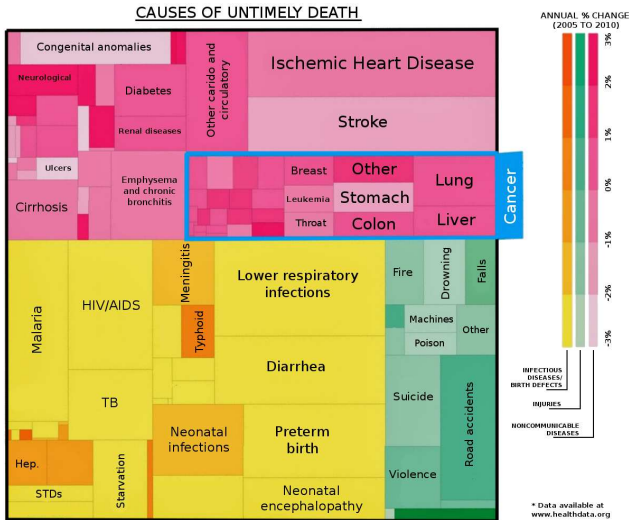
University of Wisconsin-Madison

ingle@wisc.edu

July 30, 2015

- Motivation
- Shear Wave Elastography
- Specific Aims
 - 2D Shear Wave Imaging
 - Plane Wave Imaging
 - 3D Reconstruction Algorithms
 - Experimental Validation
- Concluding Remarks

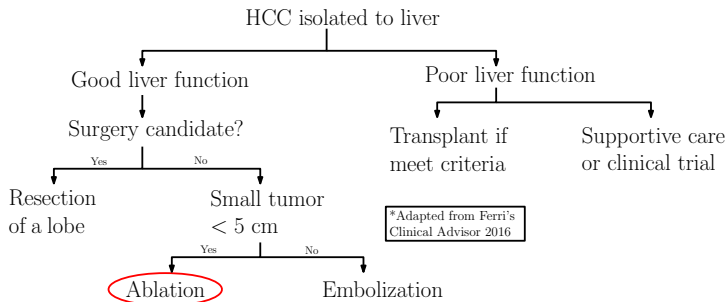
Motivation



- Bill Gates's graph of the year (The Washington Post, Dec. 2013)

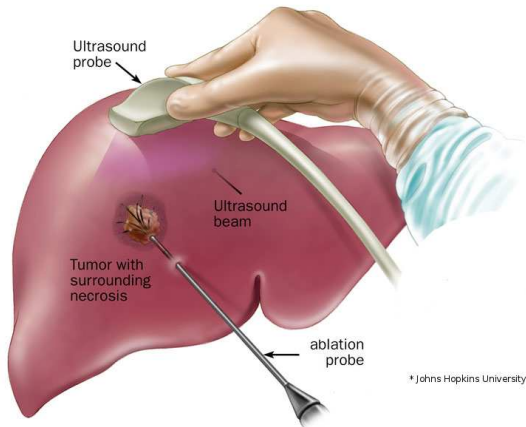
Motivation

- Hepatocellular carcinoma (HCC) is a common form of cancer with a very high mortality index of 95% and almost 750k deaths reported worldwide in 2012.
- It has a higher incidence in the less developed regions of the world with over 80% of the cases reported in Asia and Africa.
- Surgery may be used to remove a lobe of the liver. Success in such procedures depends on good liver function.



Motivation

- Ablation using RF electrode or microwave antenna is a minimally invasive procedure for treating tumors.
- This procedure does not require prolonged hospitalization and has lower morbidity as compared to surgery.



Motivation

- In order to prevent recurrence, it is crucial to design the ablation therapy so that the right volume of tissue is ablated to include a safety margin around the tumor.
- CT or MRI scans are typically performed before and after the procedure.
- B-mode ultrasound is currently used for guiding the ablation needle into the tumor.
- **The goal of this dissertation is to develop ultrasound-based stiffness estimation algorithms for liver ablation monitoring.**
- This will be a significant advancement because ultrasound imaging is potentially
 - faster than CT/MRI,
 - safer than ionizing radiation,
 - inexpensive, portable and electromagnetically compatible.

Motivation

- In order to prevent recurrence, it is crucial to design the ablation therapy so that the right volume of tissue is ablated to include a safety margin around the tumor.
- CT or MRI scans are typically performed before and after the procedure.
- B-mode ultrasound is currently used for guiding the ablation needle into the tumor.
- **The goal of this dissertation is to develop ultrasound-based stiffness estimation algorithms for liver ablation monitoring.**
- This will be a significant advancement because ultrasound imaging is potentially
 - faster than CT/MRI,
 - safer than ionizing radiation,
 - inexpensive, portable and electromagnetically compatible.

Motivation

- In order to prevent recurrence, it is crucial to design the ablation therapy so that the right volume of tissue is ablated to include a safety margin around the tumor.
- CT or MRI scans are typically performed before and after the procedure.
- B-mode ultrasound is currently used for guiding the ablation needle into the tumor.
- **The goal of this dissertation is to develop ultrasound-based stiffness estimation algorithms for liver ablation monitoring.**
- This will be a significant advancement because ultrasound imaging is potentially
 - faster than CT/MRI,
 - safer than ionizing radiation,
 - inexpensive, portable and electromagnetically compatible.

Motivation

- In order to prevent recurrence, it is crucial to design the ablation therapy so that the right volume of tissue is ablated to include a safety margin around the tumor.
- CT or MRI scans are typically performed before and after the procedure.
- B-mode ultrasound is currently used for guiding the ablation needle into the tumor.
- **The goal of this dissertation is to develop ultrasound-based stiffness estimation algorithms for liver ablation monitoring.**
- This will be a significant advancement because ultrasound imaging is potentially
 - faster than CT/MRI,
 - safer than ionizing radiation,
 - inexpensive, portable and electromagnetically compatible.

Motivation

- In order to prevent recurrence, it is crucial to design the ablation therapy so that the right volume of tissue is ablated to include a safety margin around the tumor.
- CT or MRI scans are typically performed before and after the procedure.
- B-mode ultrasound is currently used for guiding the ablation needle into the tumor.
- **The goal of this dissertation is to develop ultrasound-based stiffness estimation algorithms for liver ablation monitoring.**
- This will be a significant advancement because ultrasound imaging is potentially
 - faster than CT/MRI,
 - safer than ionizing radiation,
 - inexpensive, portable and electromagnetically compatible.

Electrode Vibration Shear Wave Elastography

- Elastography is a medical imaging method for mapping mechanical properties of tissue (such as displacement, strain, stiffness modulus, or other elasticity parameters).
- An elastography system has three main components:
 - (a) a method for producing displacements
 - (b) a method for measuring displacements
 - (c) a method for postprocessing to infer elastic properties.
- In electrode vibration elastography:
 - (a) a shear wave pulse is produced by vibrating the ablation needle
 - (b) displacements are measured using ultrasound images (cross-correlation)
 - (c) shear wave velocity is inferred by tracking the wave through the ultrasound image movie.
- A shear wave is a transverse mechanical wave; particles move perpendicular to the direction of travel of the wave.
- The wave travels faster in stiffer tissue than softer tissue, and hence shear wave velocity information can be used to distinguish treated tissue from healthy tissue.

Electrode Vibration Shear Wave Elastography

- Elastography is a medical imaging method for mapping mechanical properties of tissue (such as displacement, strain, stiffness modulus, or other elasticity parameters).
- An elastography system has three main components:
 - (a) a method for producing displacements
 - (b) a method for measuring displacements
 - (c) a method for postprocessing to infer elastic properties.
- In electrode vibration elastography:
 - (a) a shear wave pulse is produced by vibrating the ablation needle
 - (b) displacements are measured using ultrasound images (cross-correlation)
 - (c) shear wave velocity is inferred by tracking the wave through the ultrasound image movie.
- A shear wave is a transverse mechanical wave; particles move perpendicular to the direction of travel of the wave.
- The wave travels faster in stiffer tissue than softer tissue, and hence shear wave velocity information can be used to distinguish treated tissue from healthy tissue.

Electrode Vibration Shear Wave Elastography

- Elastography is a medical imaging method for mapping mechanical properties of tissue (such as displacement, strain, stiffness modulus, or other elasticity parameters).
- An elastography system has three main components:
 - (a) a method for producing displacements
 - (b) a method for measuring displacements
 - (c) a method for postprocessing to infer elastic properties.
- In electrode vibration elastography:
 - (a) a shear wave pulse is produced by vibrating the ablation needle
 - (b) displacements are measured using ultrasound images (cross-correlation)
 - (c) shear wave velocity is inferred by tracking the wave through the ultrasound image movie.
- A shear wave is a transverse mechanical wave; particles move perpendicular to the direction of travel of the wave.
- The wave travels faster in stiffer tissue than softer tissue, and hence shear wave velocity information can be used to distinguish treated tissue from healthy tissue.

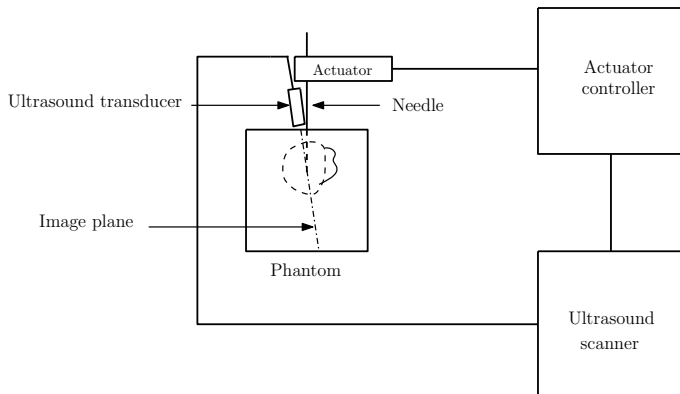
Electrode Vibration Shear Wave Elastography

- Elastography is a medical imaging method for mapping mechanical properties of tissue (such as displacement, strain, stiffness modulus, or other elasticity parameters).
- An elastography system has three main components:
 - (a) a method for producing displacements
 - (b) a method for measuring displacements
 - (c) a method for postprocessing to infer elastic properties.
- In electrode vibration elastography:
 - (a) a shear wave pulse is produced by vibrating the ablation needle
 - (b) displacements are measured using ultrasound images (cross-correlation)
 - (c) shear wave velocity is inferred by tracking the wave through the ultrasound image movie.
- A shear wave is a transverse mechanical wave; particles move perpendicular to the direction of travel of the wave.
- The wave travels faster in stiffer tissue than softer tissue, and hence shear wave velocity information can be used to distinguish treated tissue from healthy tissue.

Electrode Vibration Shear Wave Elastography

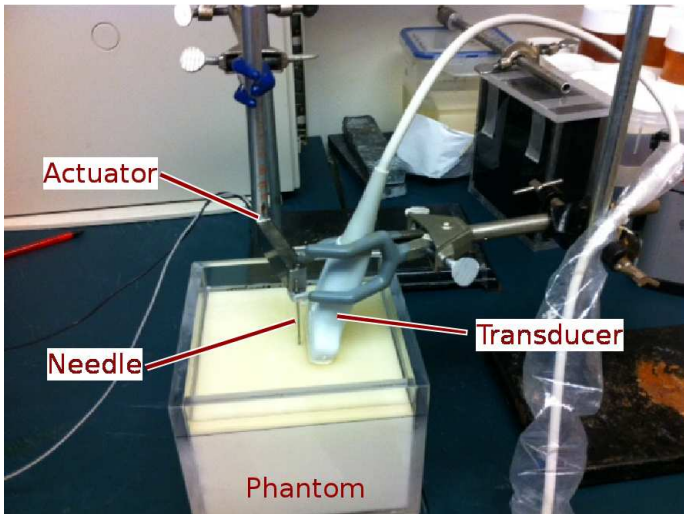
- Elastography is a medical imaging method for mapping mechanical properties of tissue (such as displacement, strain, stiffness modulus, or other elasticity parameters).
- An elastography system has three main components:
 - (a) a method for producing displacements
 - (b) a method for measuring displacements
 - (c) a method for postprocessing to infer elastic properties.
- In electrode vibration elastography:
 - (a) a shear wave pulse is produced by vibrating the ablation needle
 - (b) displacements are measured using ultrasound images (cross-correlation)
 - (c) shear wave velocity is inferred by tracking the wave through the ultrasound image movie.
- A shear wave is a transverse mechanical wave; particles move perpendicular to the direction of travel of the wave.
- The wave travels faster in stiffer tissue than softer tissue, and hence shear wave velocity information can be used to distinguish treated tissue from healthy tissue.

Electrode Vibration Shear Wave Elastography

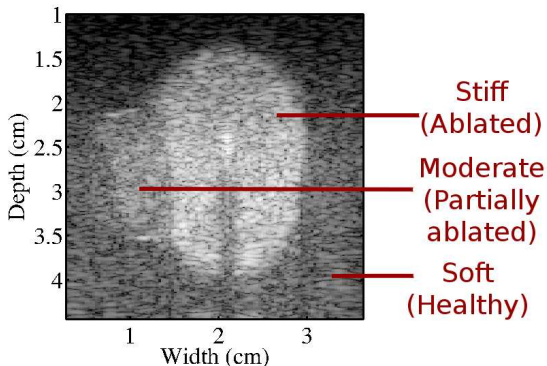


- Block diagram of the data acquisition system.

Electrode Vibration Shear Wave Elastography



Electrode Vibration Shear Wave Elastography

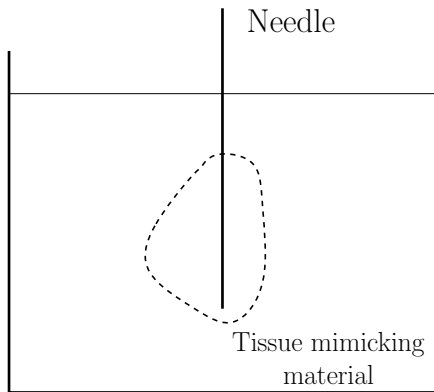


- The B-mode contrast seen in the phantom is artificial. In reality, stiffness variations are not so easily visible on B-mode.

Data Acquisition System

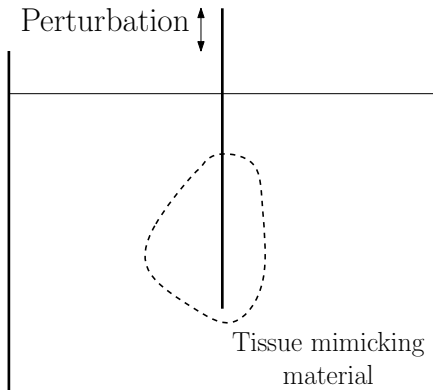
- The data acquisition system consists of a research ultrasound scanner with a programmable imaging sequence that runs in synchronization with the actuator motion.
- A linear array transducer is used for imaging at a center frequency of around 4 to 9 MHz.
- The acquisition routines are written in C++ using the manufacturers' APIs, and a user interface is designed using Qt.
- Phantom construction: oil-in-gelatin dispersion (Madsen et al.)
- Phantom stiffnesses: 10 to 40 kPa (measured using an 'ELF' mechanical tester)
- Actuator (Physik Instrumente), generates 100 micron pulses, about 30 ms wide.

Electrode Vibration Shear Wave Elastography



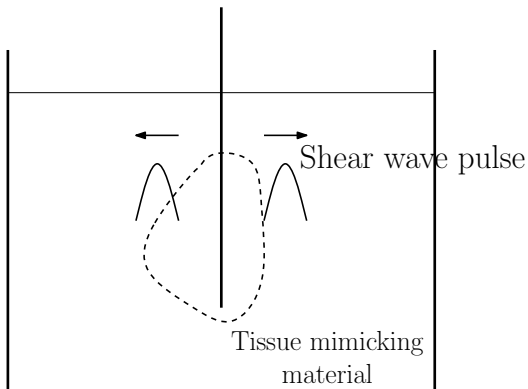
- Schematic showing essential components of an electrode vibration elastography setup.

Electrode Vibration Shear Wave Elastography



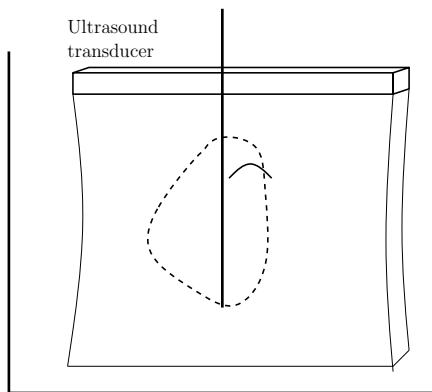
- Schematic showing essential components of an electrode vibration elastography setup.

Electrode Vibration Shear Wave Elastography



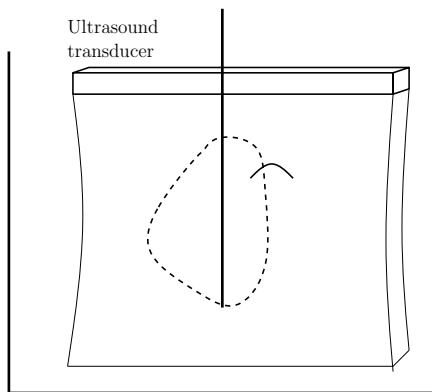
- Schematic showing essential components of an electrode vibration shear wave elastography setup.

Electrode Vibration Shear Wave Elastography



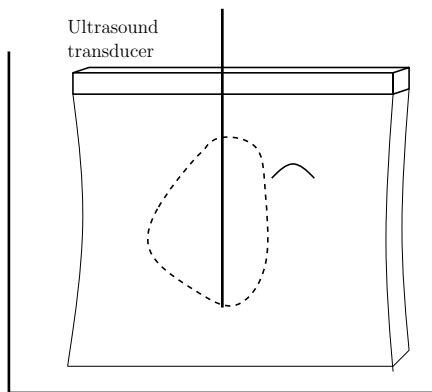
Ultrasound data frame 1

Electrode Vibration Shear Wave Elastography



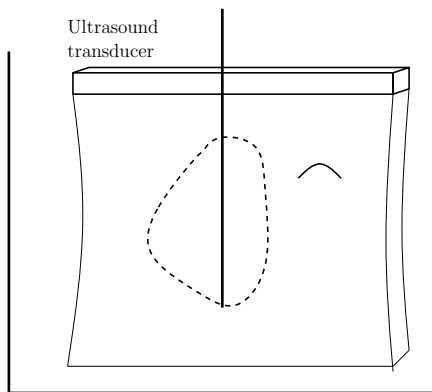
Ultrasound data frame 2

Electrode Vibration Shear Wave Elastography



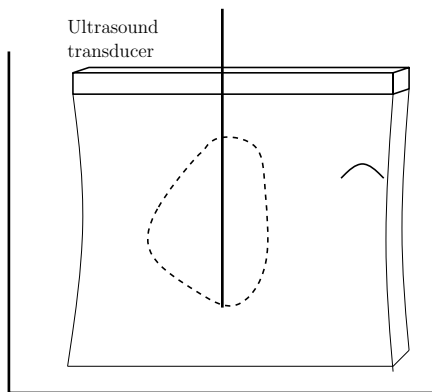
Ultrasound data frame 3

Electrode Vibration Shear Wave Elastography



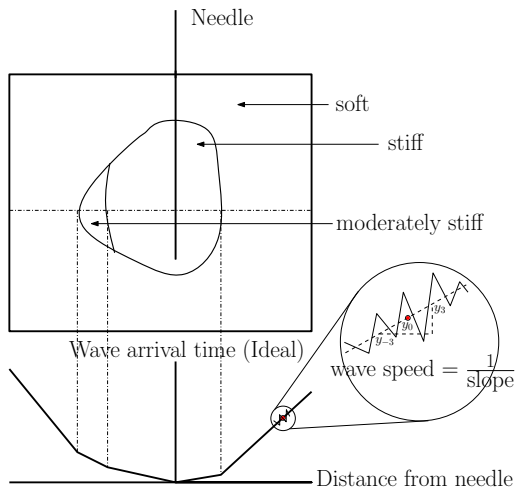
Ultrasound data frame 4

Electrode Vibration Shear Wave Elastography



... Ultrasound data frame n

Electrode Vibration Shear Wave Elastography



- Time of arrival plots are obtained by tracking the wave pulse at each depth.

Specific Aims

Aim 1

Implement a high frame rate plane wave imaging sequence for electrode vibration elastography.

Aim 2

Develop and analyze shear wave velocity reconstruction algorithms for 2D electrode vibration elastography.

Aim 3

Develop 3D reconstruction and visualization algorithms using 2D shear wave velocity information.

Aim 4

Demonstrate the use of shear wave tracking algorithms using experimental data.

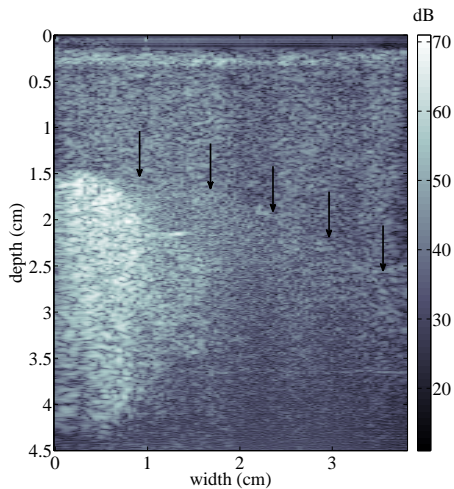
Aim 1

Implement a high frame rate plane wave imaging sequence for electrode vibration elastography.

Plane Wave Imaging

- Many snapshots of the imaging plane must be acquired at a high frame rate to track a shear wave pulse.
- Traditionally, sequentially focussed ultrasound has been used which provides very low frame rates.
- Plane wave insonification has gained popularity because it can provide very high frame rates, limited only by the speed of sound ($\sim 10\text{k}$ frames/s at 7.5 cm depth).
- The entire imaging plane is insonified hence a full dataset can be acquired with a single shear wave pulse.
- However, this results in peculiar “ghost displacement” artifacts in shear wave imaging due to poor lateral resolution [Montaldo et al. IEEE UFFC 2009].

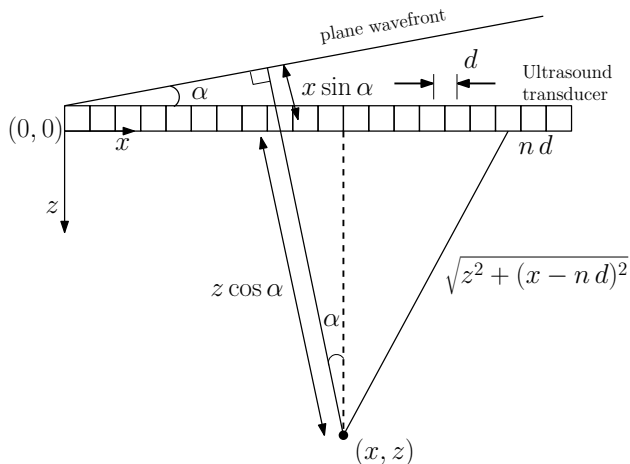
Plane Wave Imaging



Angular Compounding

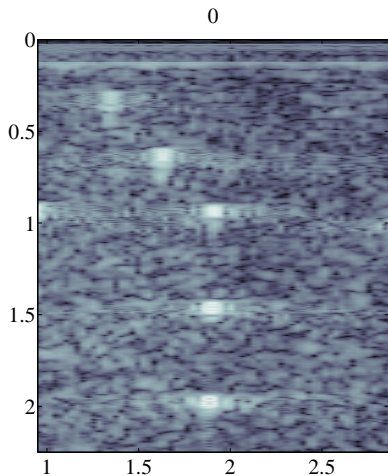
- Lateral resolution and SNR can be improved by compounding multiple angular plane wave insonifications.
- Each angular transmit is beamformed using a delay-sum technique by coherently summing up the echo signals.
- This requires calculation of the path length and time delays for each pixel in the image plane.
- The beamformed frames for different angles are averaged to produce a compounded plane wave image.
- This reduces effective frame rate by a factor equal to the number of angles used.

Angular Compounding



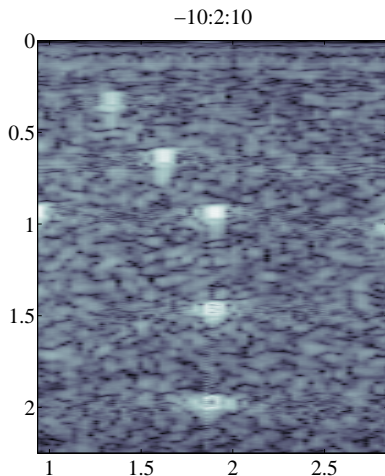
- Geometrical path length calculations used for delay-sum beamforming.

Angular Compounding



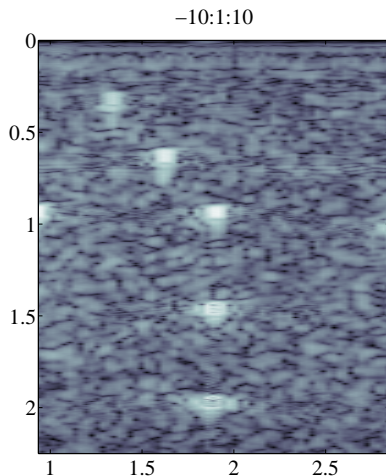
- Effect of different number of angles used for plane wave compounding.

Angular Compounding



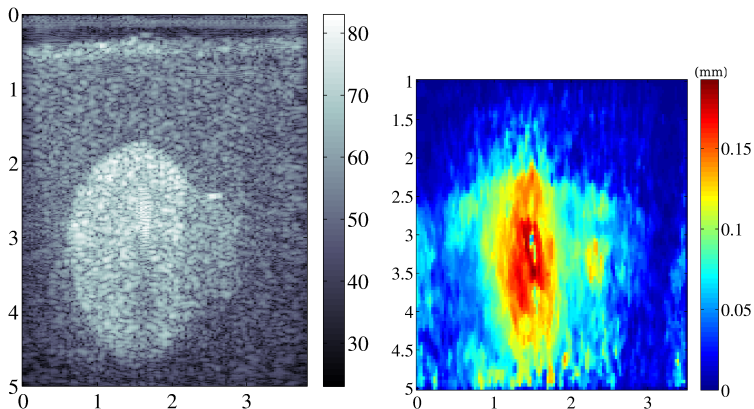
- Effect of different number of angles used for plane wave compounding.

Angular Compounding



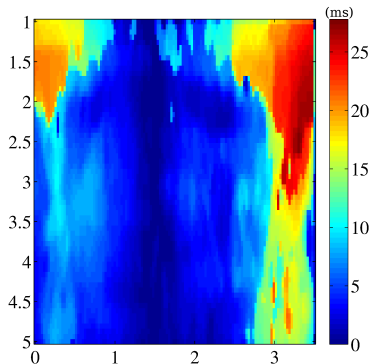
- Effect of different number of angles used for plane wave compounding.

Experimental Results



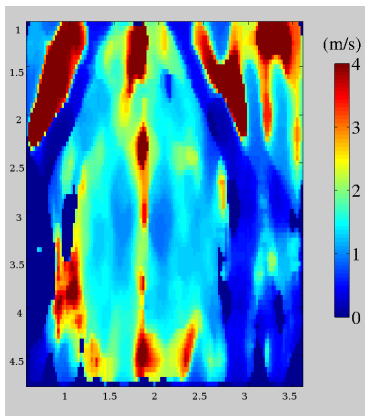
- B-mode image (left) and maximum displacement image (right) generated from angular compounded plane wave data. Note the reduction in haze artifact in the B-mode image.

Experimental Results



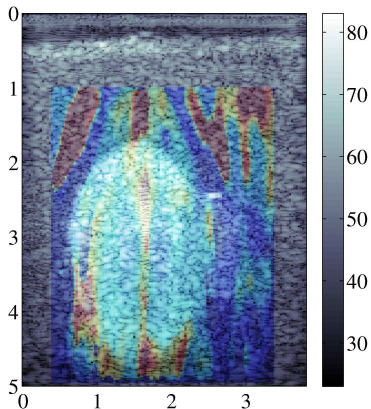
- Shear wave arrival time and velocity images generated from angular compounded plane wave data.

Experimental Results



- Shear wave arrival time and velocity images generated from angular compounded plane wave data.

Experimental Results



- Shear wave arrival time and velocity images generated from angular compounded plane wave data.

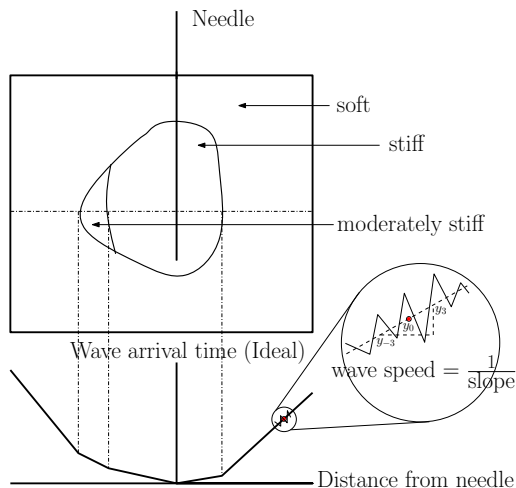
Summary

- A method for high frame rate acquisition using plane wave insonification was designed for electrode vibration elastography.
- A prototype was implemented using a research ultrasound scanner.
- Angular compounding was used to improve lateral resolution and SNR.
- With a few angular insonifications and delay-sum beamforming, a shear wave pulse can be successfully tracked over a wide field of view.

Aim 2

Develop and analyze shear wave velocity reconstruction algorithms for 2D electrode vibration shear wave elastography.

Recall: Noisy Time of Arrival Data

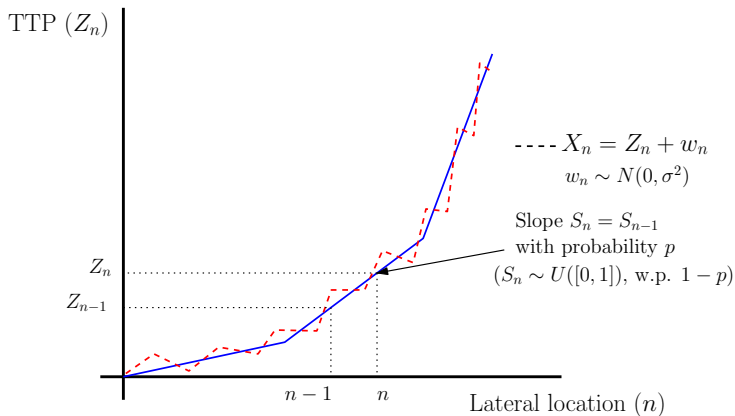


- The goal of a filtering algorithm is to estimate local slope values from noisy data.

Hidden Markov Model

- The piecewise linear function has unknown number and locations of changepoints.
- We model the noisy time of arrival data as an hidden Markov model (HMM).
- An HMM is a stochastic model that consists of a system that evolves “behind the curtain” according to a certain rule, and the observer sees a distorted version of the output of this system.
- More precisely, the model has a “state transition function” and an “observation function.”

Hidden Markov Model



Random variables used for defining the HMM.

Hidden Markov Model

Our goals are twofold now:

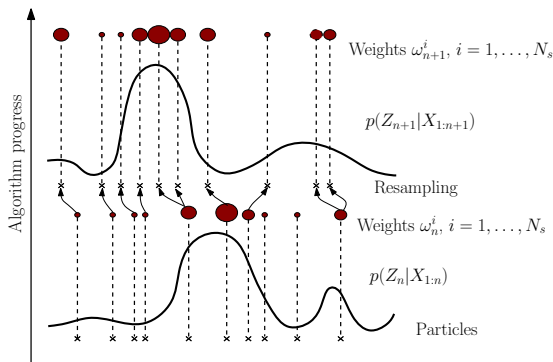
- Select sensible values for model parameters (ρ, σ^2) .
- Find the most sensible values for slopes $S_{1:N}$ using data $X_{1:N}$.

We propose two different algorithms to estimate the slope values:

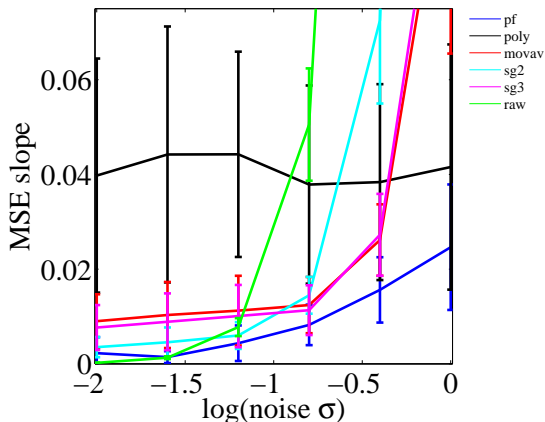
- Particle filter, operating on a continuous state space.
- MAPSLOPE-FASTTRELLIS, operating on a discretized state space.

Particle Filter

- Particle filtering is a Monte-Carlo technique for smoothing noisy data by estimating the posterior density $p(Z_n|X_{0:n})$.
- The density is approximated via a large number of “particles” in the state space: $p(Z_n|X_{0:n}) = \sum_{i=1}^{N_s} \omega_n^i \delta(Z_n - Z_n^i)$.
- Knowing $p(Z_n|X_{0:n})$, we can calculate various state estimators (maximum likelihood, mean, median, ...)

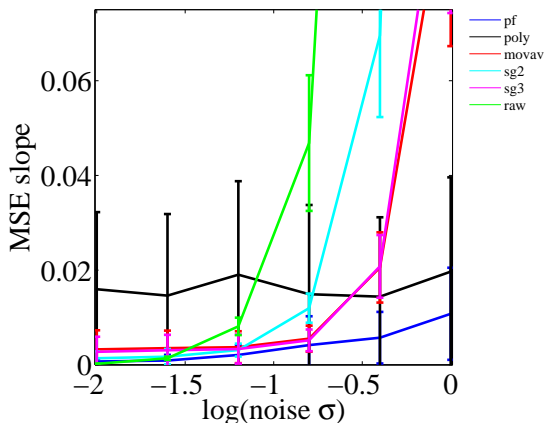


Simulation Results



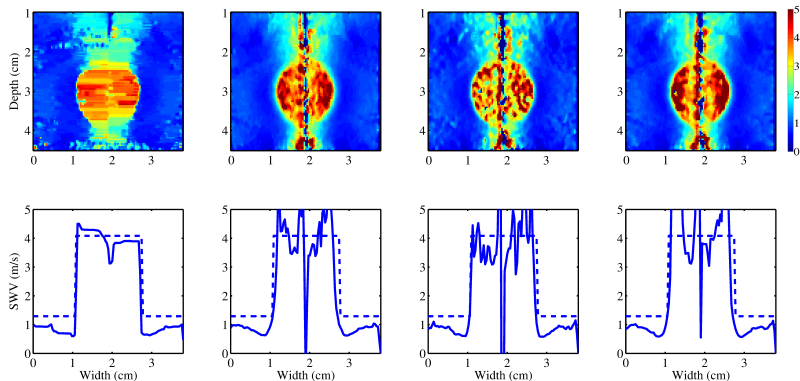
- Synthetic piecewise linear data with slopes between $[0, 1]$ and additive Gaussian noise was filtered with different algorithms. Reconstruction MSE is shown for $p = 0.85$ at different noise levels.

Simulation Results



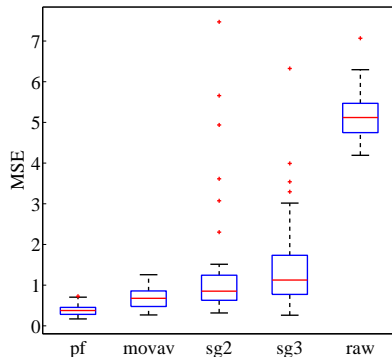
- Synthetic piecewise linear data with slopes between $[0, 1]$ and additive Gaussian noise was filtered with different algorithms. Reconstruction MSE is shown for $p = 0.95$ at different noise levels.

Finite Element Simulation Results



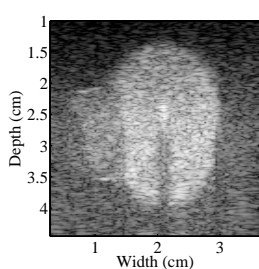
- Shear wave velocity reconstruction profiles using (a) particle filter (b) moving average (c) 2nd order Savitzky-Golay and (d) 3rd order Savitzky-Golay filters [Ingle, Varghese 2015 (under review)]

Finite Element Simulation MSE Results

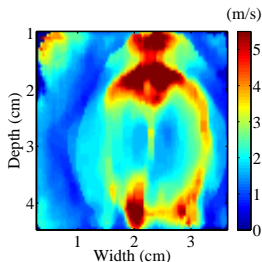


- Mean squared error in slope values estimated using the particle filter compared to other standard slope estimation methods.

Experimental Results



(a) B-mode



(b) Particle filter

- B-mode image of the phantom with corresponding SWV map reconstructed using the particle filtering algorithm [Ingle, Varghese, IEEE ISBI 2013]

Experimental Results

ROI	Shear wave velocity	
	SWV (m/s)	
	Particle Filter	Direct Measurement
Inclusion	3.8 ± 2.2	2.8 ± 1.1
Partially Ablated	2.0 ± 0.2	2.3 ± 0.8
Background	1.3 ± 0.2	1.3 ± 0.4

Method	Inclusion areas in cm^2	
	Phantom-1	Phantom-2
Particle filter	4.45 ± 0.15	4.13 ± 0.18
Least squares	4.11 ± 0.19	4.01 ± 0.14
B-Mode (truth)	4.68 ± 0.14	4.47 ± 0.11

- A faster algorithm than particle filtering can be designed by discretizing the state space (slope values).
- Let $\mathcal{S} = \{0, \frac{1}{M-1}, \frac{2}{M-1}, \dots, 1\}$ the set of M quantized slope values, $|\mathcal{S}| = M$.
- Assuming p, σ^2 are known, a maximum a posteriori (MAP) estimate of the slope sequence can be obtained as

$$\begin{aligned}(\hat{s}_1, \dots, \hat{s}_N) &= \arg \max_{(s_1, \dots, s_N) \in \mathcal{S}^N} \log p(Z_1, \dots, Z_N | X_1, \dots, X_N) \\ &= \arg \max_{(s_1, \dots, s_N) \in \mathcal{S}^N} \sum_{i=1}^N [\log p(z_i | z_{i-1}, z_{i-2}) + \log p(x_i | z_i)].\end{aligned}$$

- Combinatorially, there are M^N possible slope sequences to check.
- MATLAB implementation runs in $\mathcal{O}(M^2 N^3)$ time using dynamic programming.

- A faster algorithm than particle filtering can be designed by discretizing the state space (slope values).
- Let $\mathcal{S} = \{0, \frac{1}{M-1}, \frac{2}{M-1}, \dots, 1\}$ the set of M quantized slope values, $|\mathcal{S}| = M$.
- Assuming p, σ^2 are known, a maximum a posteriori (MAP) estimate of the slope sequence can be obtained as

$$\begin{aligned}(\hat{s}_1, \dots, \hat{s}_N) &= \arg \max_{(s_1, \dots, s_N) \in \mathcal{S}^N} \log p(Z_1, \dots, Z_N | X_1, \dots, X_N) \\ &= \arg \max_{(s_1, \dots, s_N) \in \mathcal{S}^N} \sum_{i=1}^N [\log p(z_i | z_{i-1}, z_{i-2}) + \log p(x_i | z_i)].\end{aligned}$$

- Combinatorially, there are M^N possible slope sequences to check.
- MATLAB implementation runs in $\mathcal{O}(M^2 N^3)$ time using dynamic programming.

- A faster algorithm than particle filtering can be designed by discretizing the state space (slope values).
- Let $\mathcal{S} = \{0, \frac{1}{M-1}, \frac{2}{M-1}, \dots, 1\}$ the set of M quantized slope values, $|\mathcal{S}| = M$.
- Assuming p, σ^2 are known, a maximum a posteriori (MAP) estimate of the slope sequence can be obtained as

$$\begin{aligned}(\hat{s}_1, \dots, \hat{s}_N) &= \arg \max_{(s_1, \dots, s_N) \in \mathcal{S}^N} \log p(Z_1, \dots, Z_N | X_1, \dots, X_N) \\ &= \arg \max_{(s_1, \dots, s_N) \in \mathcal{S}^N} \sum_{i=1}^N [\log p(z_i | z_{i-1}, z_{i-2}) + \log p(x_i | z_i)].\end{aligned}$$

- Combinatorially, there are M^N possible slope sequences to check.
- MATLAB implementation runs in $\mathcal{O}(M^2 N^3)$ time using dynamic programming.

- A faster algorithm than particle filtering can be designed by discretizing the state space (slope values).
- Let $\mathcal{S} = \{0, \frac{1}{M-1}, \frac{2}{M-1}, \dots, 1\}$ the set of M quantized slope values, $|\mathcal{S}| = M$.
- Assuming p, σ^2 are known, a maximum a posteriori (MAP) estimate of the slope sequence can be obtained as

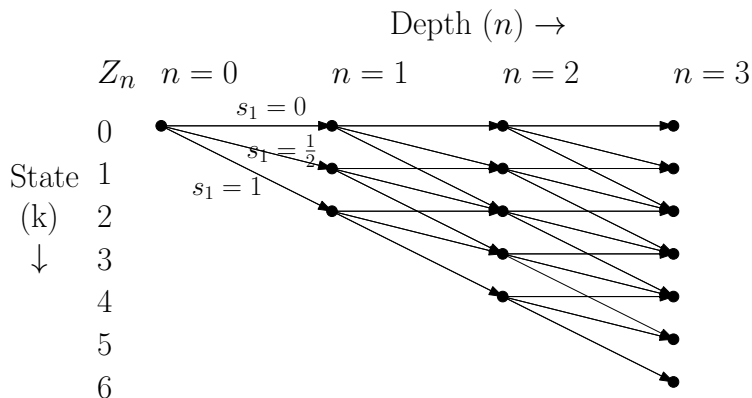
$$\begin{aligned}(\hat{s}_1, \dots, \hat{s}_N) &= \arg \max_{(s_1, \dots, s_N) \in \mathcal{S}^N} \log p(Z_1, \dots, Z_N | X_1, \dots, X_N) \\ &= \arg \max_{(s_1, \dots, s_N) \in \mathcal{S}^N} \sum_{i=1}^N [\log p(z_i | z_{i-1}, z_{i-2}) + \log p(x_i | z_i)].\end{aligned}$$

- Combinatorially, there are M^N possible slope sequences to check.
- MATLAB implementation runs in $\mathcal{O}(M^2 N^3)$ time using dynamic programming.

- A faster algorithm than particle filtering can be designed by discretizing the state space (slope values).
- Let $\mathcal{S} = \{0, \frac{1}{M-1}, \frac{2}{M-1}, \dots, 1\}$ the set of M quantized slope values, $|\mathcal{S}| = M$.
- Assuming p, σ^2 are known, a maximum a posteriori (MAP) estimate of the slope sequence can be obtained as

$$\begin{aligned}(\hat{s}_1, \dots, \hat{s}_N) &= \arg \max_{(s_1, \dots, s_N) \in \mathcal{S}^N} \log p(Z_1, \dots, Z_N | X_1, \dots, X_N) \\ &= \arg \max_{(s_1, \dots, s_N) \in \mathcal{S}^N} \sum_{i=1}^N [\log p(z_i | z_{i-1}, z_{i-2}) + \log p(x_i | z_i)].\end{aligned}$$

- Combinatorially, there are M^N possible slope sequences to check.
- MATLAB implementation runs in $\mathcal{O}(M^2 N^3)$ time using dynamic programming.



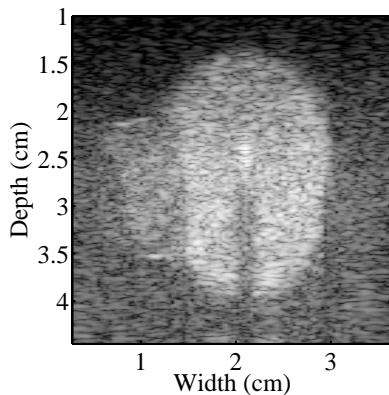
- A trellis structure shown up to a depth of 3, with 3 distinct slope values.
- A dynamic program finds the optimal path on this trellis to maximize the posterior density $\sum_{i=1}^N [\log p(z_i | z_{i-1}, z_{i-2}) + \log p(x_i | z_i)]$.

We propose an automatic method to choose (p, σ^2) using an alternating-maximization algorithm MAPSLOPE [Ingle et al., Asilomar 2014/Sig. Proc. 2015].

MAPSLOPE Algorithm

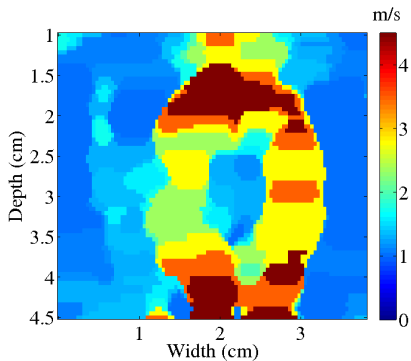
- 1 Start with an initial guess for (p, σ^2) .
- 2 Loop
 - 1 Run FASTTRELLIS(p, σ^2) to estimate slope sequence.
 - 2 Estimate new $p^* = \frac{\text{\#times slope stays constant}}{\text{\#data points}}$
 - 3 Estimate new $\sigma^{*2} = \text{var}(\text{noisy data} - \text{current fit})$
 - 4 $p \leftarrow p^*, \sigma^2 \leftarrow \sigma^{*2}$
- 3 Stop if some convergence criterion is met.

Experimental Results



B-mode image of the phantom inclusion.

Experimental Results



Corresponding shear wave velocity image.

Experimental Results

Slowness and Stiffness estimates			
	Stiff	Intermediate	Soft
Velocity (m/s)	3.09 ± 0.9	2.03 ± 0.35	1.21 ± 0.29
SNR dB (SWV)	12.6 ± 3.7	17.6 ± 3.4	12.7 ± 1.9

Values of shear wave slowness, shear wave velocity and Young's modulus for the three different regions in the experimental phantom obtained from the MAPSLOPE algorithm are indicated.

Summary

- A stochastic model for noisy arrival time (piecewise linear) data was developed.
- The particle filter algorithm provides better mean squared reconstruction error than standard slope estimation algorithms (such as moving average or Savitzky-Golay).
- A faster algorithm that uses dynamic programming and has provable convergence properties was also developed.
- Shear wave velocity measurements from these algorithms also agreed with direct mechanical measurement.

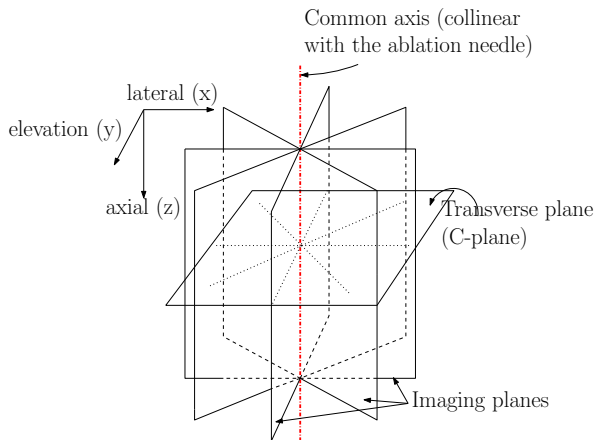
Aim 3

Develop 3D reconstruction and visualization algorithms using 2D shear wave velocity information.

Sheaf Acquisition

- 2D shear wave velocity reconstruction algorithms can be extended to 3D by acquiring multiple planes of data in a sheaf geometry.
- A sheaf is a collection of planes that intersect in a line.
- With the knowledge of shear wave velocity values on every plane in the sheaf, shear wave velocity values are estimated over each transverse “C-plane”.
- Shear wave velocity values are reconstructed on a fine grid on each C-plane.
- A stack of these C-planes can be used to generate a 3D visualization.

Sheaf Acquisition



- Diagram showing the orientation of the image planes and a C-plane in a sheaf.

3D Reconstruction

- Given a set of (noisy) data points on each transverse plane, we would like to infer the shear wave velocity values on a grid and display it as a volume.
- The reconstruction should satisfy these intuitive requirements:
 - ① It must “agree” with the known data points at the scattered locations, i.e. the known data points should be close to the **interpolation** from the nearest grid points.
 - ② It should look “pleasing” i.e. **smoothness**.
- This may be ill-posed because the number of data points is often much smaller than the number of grid points i.e. more unknowns than known data points.

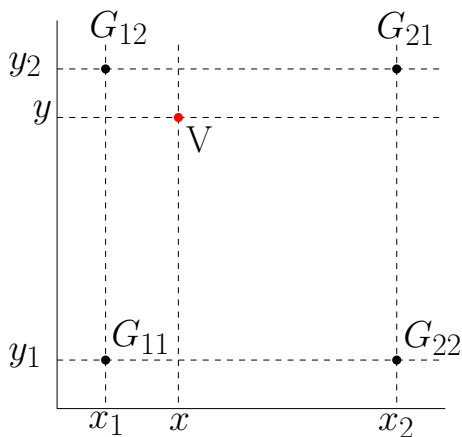
3D Reconstruction

- Given a set of (noisy) data points on each transverse plane, we would like to infer the shear wave velocity values on a grid and display it as a volume.
- The reconstruction should satisfy these intuitive requirements:
 - ① It must “agree” with the known data points at the scattered locations, i.e. the known data points should be close to the **interpolation** from the nearest grid points.
 - ② It should look “pleasing” i.e. **smoothness**.
- This may be ill-posed because the number of data points is often much smaller than the number of grid points i.e. more unknowns than known data points.

3D Reconstruction

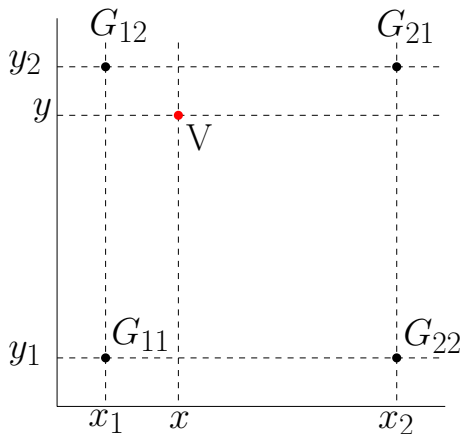
- Given a set of (noisy) data points on each transverse plane, we would like to infer the shear wave velocity values on a grid and display it as a volume.
- The reconstruction should satisfy these intuitive requirements:
 - ① It must “agree” with the known data points at the scattered locations, i.e. the known data points should be close to the **interpolation** from the nearest grid points.
 - ② It should look “pleasing” i.e. **smoothness**.
- This may be ill-posed because the number of data points is often much smaller than the number of grid points i.e. more unknowns than known data points.

Requirement 1: Interpolation



- We use bilinear interpolation so that each data point (V) is a linear combination of the (unknown) function values (G) at the eight neighbors on the grid.

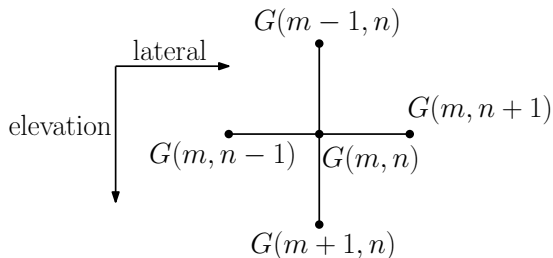
Requirement 1: Interpolation



- Value at red dot \equiv linear combination involving 4 grid neighbors

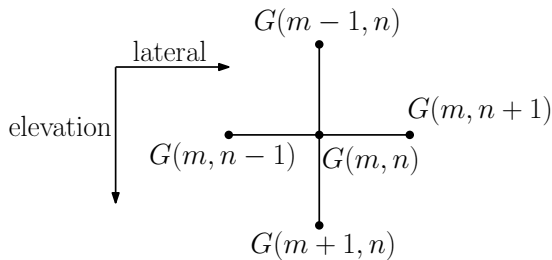
Requirement 2: Smoothness

- We enforce smoothness by constraining the Laplacian calculated on the grid through finite differencing.



Requirement 2: Smoothness

- We enforce smoothness by constraining the Laplacian calculated on the grid through finite differencing.



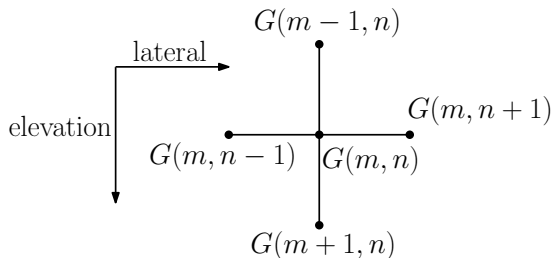
$$\frac{d^2 G}{dx^2}(m, n) \approx \frac{1}{2}(G(m+1, n) - G(m-1, n) + 2G(m, n))$$

$$\frac{d^2 G}{dy^2}(m, n) \approx \frac{1}{2}(G(m, n+1) - G(m, n-1) + 2G(m, n))$$

$$\nabla^2 G(m, n) = \frac{d^2 G}{dx^2}(m, n) + \frac{d^2 G}{dy^2}(m, n)$$

Requirement 2: Smoothness

- We enforce smoothness by constraining the Laplacian calculated on the grid through finite differencing.



Laplacian \equiv linear combination involving 5 grid points

Penalized Least Squares Formulation

Let

\mathbf{g} denote the vector of unknown function values on the grid

\mathbf{v} denote the vector of known data values at the scattered points

Since all requirements are linear combinations of the grid values, we can represent them in matrix form. Let

\mathbf{M} be the interpolant matrix

\mathbf{D} be the finite differencing Laplacian matrix.

By choice of \mathbf{g}

$$\text{minimize } \|\mathbf{v} - \mathbf{M}\mathbf{g}\|^2$$

subject to

$$\|\mathbf{D}\mathbf{g}\|^2 \leq c$$

where $\|\cdot\|$ denotes the 2-norm (square-root-of-sum-of-squares) and c is some user specified constant.

Penalized Least Squares Formulation

Let

\mathbf{g} denote the vector of unknown function values on the grid

\mathbf{v} denote the vector of known data values at the scattered points

Since all requirements are linear combinations of the grid values, we can represent them in matrix form. Let

\mathbf{M} be the interpolant matrix

\mathbf{D} be the finite differencing Laplacian matrix.

By choice of \mathbf{g}

$$\text{minimize } \|\mathbf{v} - \mathbf{Mg}\|^2$$

subject to

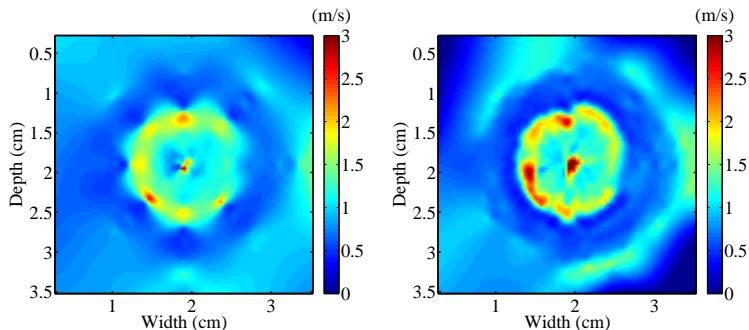
$$\|\mathbf{Dg}\|^2 \leq c$$

where $\|\cdot\|$ denotes the 2-norm (square-root-of-sum-of-squares) and c is some user specified constant.

Penalized Least Squares Formulation

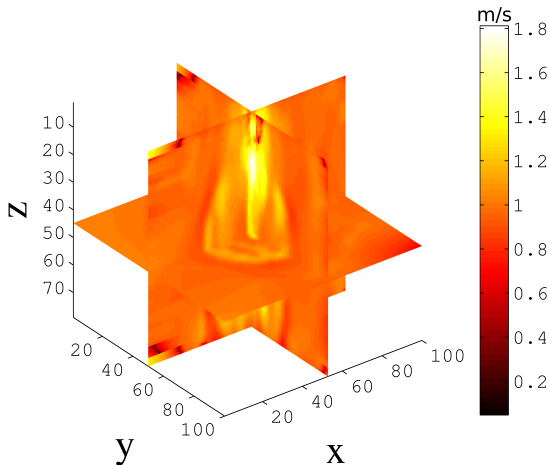
- Using a Lagrange multiplier λ the problem is reformulated as:
minimize $\|\mathbf{v} - \mathbf{M}\mathbf{g}\|^2 + \lambda\|\mathbf{D}\mathbf{g}\|^2$
 \mathbf{g}
- This has a closed form solution: $\mathbf{g} = (\mathbf{M}^T\mathbf{M} + \lambda\mathbf{D}^T\mathbf{D})^{-1}\mathbf{M}^T\mathbf{v}$.
- Here the Lagrange multiplier λ controls the amount of smoothing: smaller λ means less smoothing and vice versa.
- This smoothing parameter can be chosen in an objective manner using the method of leave-one-out crossvalidation.
- The matrix inverse is not calculated explicitly.
- This was implemented in C++ using a sparse-QR decomposition routine.

C-Plane Results



- Two transverse plane reconstructions shown over a plane at a depth of 3 cm. (a) was reconstructed using 4 image planes while (b) was reconstructed with 6 image planes. There is considerably more “detail” visible in (b) whereas the reconstruction in (a) is smoother.

Experimental Results



- A 3D-slice view of the reconstruction of the ablation phantom [Ingle, Varghese, IEEE TMI 2014],[Ingle et al., IEEE EMBC 2014]

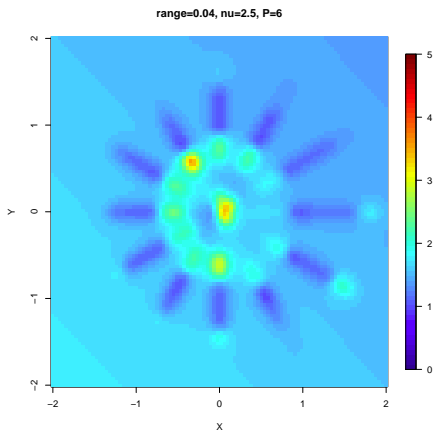
Experimental Results

Shear wave velocity estimates in m/s

	4 image planes	16 image planes	Direct Measurement
background	0.75 ± 0.08	0.75 ± 0.08	0.9 ± 0.07
irregular region	1.02 ± 0.02	0.99 ± 0.02	1.1 ± 0.05
ellipsoid	1.26 ± 0.11	1.24 ± 0.12	1.2 ± 0.03

- The reconstructions were repeated with 4 and 16 image planes. Mean and standard deviation SWV values were calculated using three different ROIs.

Spokewheel Artifact

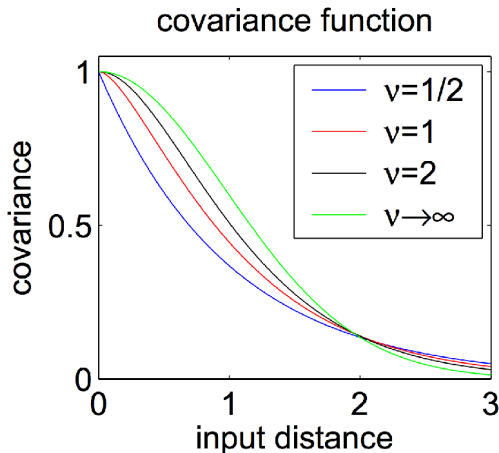


- Spokewheel artifact causes streaks along the sheaf lines.

Kernel Smoothing

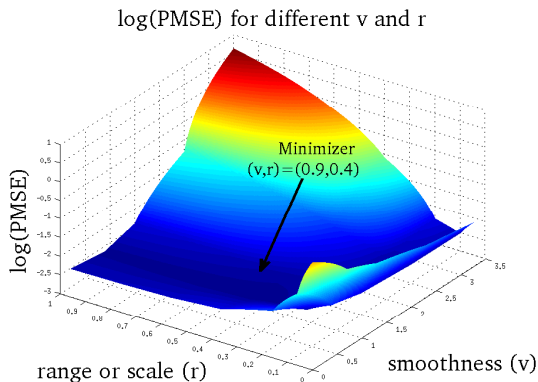
- On each C-plane, the shear wave velocity field can be represented by a function $f : \mathbb{R}^2 \rightarrow [0, \infty)$.
- Noisy point evaluations are acquired at different locations $\{t_i\}_{i=1}^n$: $u_i = f(t_i) + \epsilon_i$ each $t_i \in \mathbb{R}^2$ is situated along the radial lines.
- f is assumed to be a member of a “nice set of functions” with K as the kernel function.
- A function in this set can be expressed as a linear combination:
$$\hat{f}(t) = \sum_{i=1}^n c_i K(\|t - t_i\|).$$
- This formulation suggests that each data point t_i imposes a “region of influence” that varies with its distance from an arbitrary point t .
- The two-parameter Matérn kernel is used for getting rid of the spoke wheel artifact, with the parameters chosen in a data-adaptive manner.

Matérn Kernel



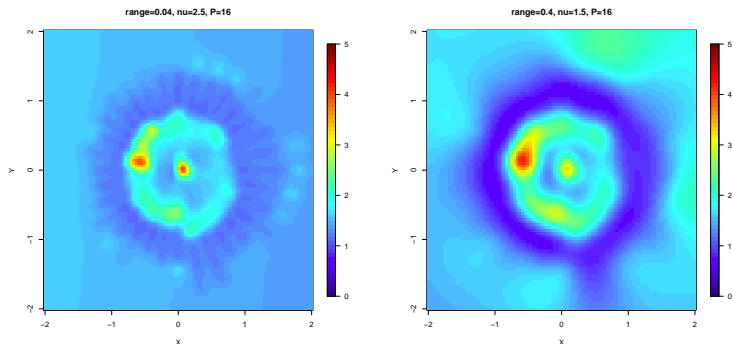
- We use the two parameter Matérn kernel which allows controlling the smoothness and range of influence of the kernel. [C. E. Rasmussen, 2006].

Choosing the Matérn Kernel Parameters



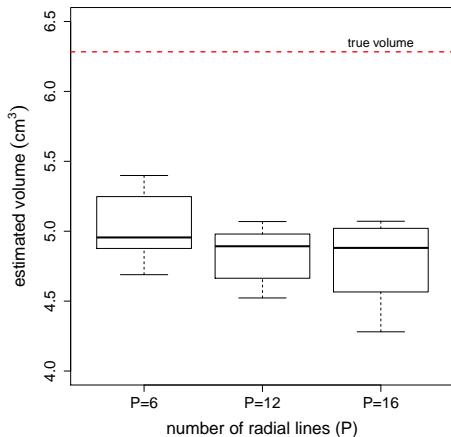
- Simulated mean squared error (MSE) performance for different values of Matérn kernel parameters. We choose the one that locally minimizes the MSE [Ingle, Varghese (in preparation)].

Results: C-plane Reconstructions



- Kernel smoothing with the right parameters gives good reconstruction quality and reduces the spokewheel artifact too.

Results: Volume Estimates



- Estimated volume is lower than the actual volume.

Full 3D Reconstruction

- It is desirable to extend the sheaf reconstruction algorithm to generate complete three dimensional visualizations of shear wave velocities.
- The intermediate step of reconstructing transverse C-planes is an approximation and is used to make the reconstruction algorithm computationally tractable.
- A commonly used fast method for 3D visualization is nearest neighbor interpolation which involves assigning the value of the closest data point to each grid node.
- Using a Markov random field model, a computationally tractable reconstruction algorithm that has better reconstruction quality than nearest neighbor interpolation is developed.

Full 3D Reconstruction

- It is desirable to extend the sheaf reconstruction algorithm to generate complete three dimensional visualizations of shear wave velocities.
- The intermediate step of reconstructing transverse C-planes is an approximation and is used to make the reconstruction algorithm computationally tractable.
- A commonly used fast method for 3D visualization is nearest neighbor interpolation which involves assigning the value of the closest data point to each grid node.
- Using a Markov random field model, a computationally tractable reconstruction algorithm that has better reconstruction quality than nearest neighbor interpolation is developed.

Full 3D Reconstruction

- It is desirable to extend the sheaf reconstruction algorithm to generate complete three dimensional visualizations of shear wave velocities.
- The intermediate step of reconstructing transverse C-planes is an approximation and is used to make the reconstruction algorithm computationally tractable.
- A commonly used fast method for 3D visualization is nearest neighbor interpolation which involves assigning the value of the closest data point to each grid node.
- Using a Markov random field model, a computationally tractable reconstruction algorithm that has better reconstruction quality than nearest neighbor interpolation is developed.

Full 3D Reconstruction

- It is desirable to extend the sheaf reconstruction algorithm to generate complete three dimensional visualizations of shear wave velocities.
- The intermediate step of reconstructing transverse C-planes is an approximation and is used to make the reconstruction algorithm computationally tractable.
- A commonly used fast method for 3D visualization is nearest neighbor interpolation which involves assigning the value of the closest data point to each grid node.
- Using a Markov random field model, a computationally tractable reconstruction algorithm that has better reconstruction quality than nearest neighbor interpolation is developed.

Markov Random Field Model

- Consider a function defined on the nodes of a 3D grid.
- A Markov random field has the property that conditioned on the function values at the neighboring nodes, the value at any given node is independent of the values at all other nodes.
- Intuitively, this means that the “region of influence” for each node in the 3D grid consists of its immediate neighbors, forming a “clique”.
- The joint density function of the values at all the grid nodes is expressed as a function of the “potential energy” of the configuration of the values at the nodes, where higher probabilities are assigned to configurations with lower potential.
- These “clique potentials” can be defined to impose a desirable structure on the final grid reconstruction.

Markov Random Field Model

- Consider a function defined on the nodes of a 3D grid.
- A Markov random field has the property that conditioned on the function values at the neighboring nodes, the value at any given node is independent of the values at all other nodes.
- Intuitively, this means that the “region of influence” for each node in the 3D grid consists of its immediate neighbors, forming a “clique”.
- The joint density function of the values at all the grid nodes is expressed as a function of the “potential energy” of the configuration of the values at the nodes, where higher probabilities are assigned to configurations with lower potential.
- These “clique potentials” can be defined to impose a desirable structure on the final grid reconstruction.

Markov Random Field Model

- Consider a function defined on the nodes of a 3D grid.
- A Markov random field has the property that conditioned on the function values at the neighboring nodes, the value at any given node is independent of the values at all other nodes.
- Intuitively, this means that the “region of influence” for each node in the 3D grid consists of its immediate neighbors, forming a “clique”.
- The joint density function of the values at all the grid nodes is expressed as a function of the “potential energy” of the configuration of the values at the nodes, where higher probabilities are assigned to configurations with lower potential.
- These “clique potentials” can be defined to impose a desirable structure on the final grid reconstruction.

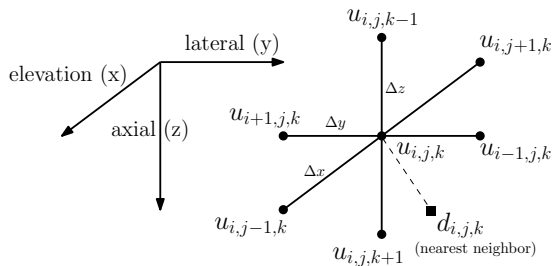
Markov Random Field Model

- Consider a function defined on the nodes of a 3D grid.
- A Markov random field has the property that conditioned on the function values at the neighboring nodes, the value at any given node is independent of the values at all other nodes.
- Intuitively, this means that the “region of influence” for each node in the 3D grid consists of its immediate neighbors, forming a “clique”.
- The joint density function of the values at all the grid nodes is expressed as a function of the “potential energy” of the configuration of the values at the nodes, where higher probabilities are assigned to configurations with lower potential.
- These “clique potentials” can be defined to impose a desirable structure on the final grid reconstruction.

Markov Random Field Model

- Consider a function defined on the nodes of a 3D grid.
- A Markov random field has the property that conditioned on the function values at the neighboring nodes, the value at any given node is independent of the values at all other nodes.
- Intuitively, this means that the “region of influence” for each node in the 3D grid consists of its immediate neighbors, forming a “clique”.
- The joint density function of the values at all the grid nodes is expressed as a function of the “potential energy” of the configuration of the values at the nodes, where higher probabilities are assigned to configurations with lower potential.
- These “clique potentials” can be defined to impose a desirable structure on the final grid reconstruction.

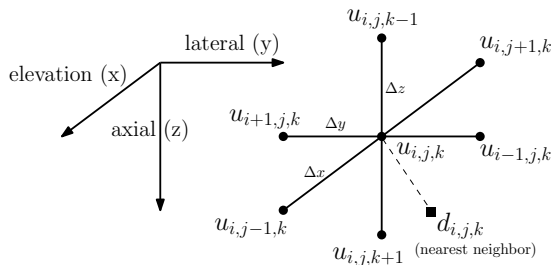
Markov Random Field Model



- The clique potential is defined using a 6-neighborhood:

$$V(u_{i,j,k}) = (u_{i,j,k} - d_{i,j,k})^2 + \lambda \left[\left(\frac{u_{i,j+1,k} + u_{i,j-1,k} - 2u_{i,j,k}}{\Delta x^2} \right)^2 + \left(\frac{u_{i+1,j,k} + u_{i-1,j,k} - 2u_{i,j,k}}{\Delta y^2} \right)^2 + \left(\frac{u_{i,j,k+1} + u_{i,j,k-1} - 2u_{i,j,k}}{\Delta z^2} \right)^2 \right]$$

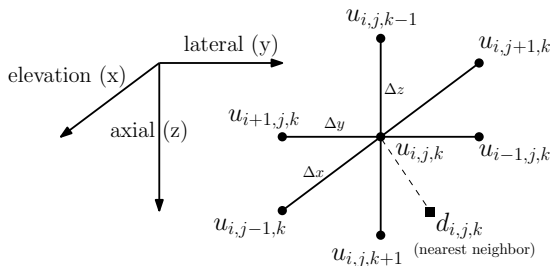
Markov Random Field Model



- Nearest neighbor difference

$$V(u_{i,j,k}) = (u_{i,j,k} - d_{i,j,k})^2 + \lambda \left[\left(\frac{u_{i,j+1,k} + u_{i,j-1,k} - 2u_{i,j,k}}{\Delta x^2} \right)^2 + \left(\frac{u_{i+1,j,k} + u_{i-1,j,k} - 2u_{i,j,k}}{\Delta y^2} \right)^2 + \left(\frac{u_{i,j,k+1} + u_{i,j,k-1} - 2u_{i,j,k}}{\Delta z^2} \right)^2 \right]$$

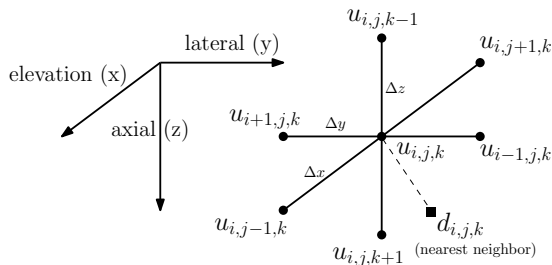
Markov Random Field Model



- Second order finite difference (derivative)

$$V(u_{i,j,k}) = (u_{i,j,k} - d_{i,j,k})^2 + \lambda \left[\left(\frac{u_{i,j+1,k} + u_{i,j-1,k} - 2u_{i,j,k}}{\Delta x^2} \right)^2 + \left(\frac{u_{i+1,j,k} + u_{i-1,j,k} - 2u_{i,j,k}}{\Delta y^2} \right)^2 + \left(\frac{u_{i,j,k+1} + u_{i,j,k-1} - 2u_{i,j,k}}{\Delta z^2} \right)^2 \right]$$

Markov Random Field Model



- Weighting factor

$$V(u_{i,j,k}) = (u_{i,j,k} - d_{i,j,k})^2 + \lambda \left[\left(\frac{u_{i,j+1,k} + u_{i,j-1,k} - 2u_{i,j,k}}{\Delta x^2} \right)^2 + \left(\frac{u_{i+1,j,k} + u_{i-1,j,k} - 2u_{i,j,k}}{\Delta y^2} \right)^2 + \left(\frac{u_{i,j,k+1} + u_{i,j,k-1} - 2u_{i,j,k}}{\Delta z^2} \right)^2 \right]$$

Markov Random Field Model

- The joint density function is defined so that “high energy” configurations have lower probability, and vice versa.
- Denoting the vector of $u_{i,j,k}$ values as \mathbf{u} , define the density function

$$p(\mathbf{u}) \propto \exp\left(-\sum_{i,j,k} V(u_{i,j,k})\right).$$

- The goal of the reconstruction algorithm is to estimate the mode of this density function, i.e., the configuration \mathbf{u} that maximizes $p(\mathbf{u})$.

Markov Random Field Model

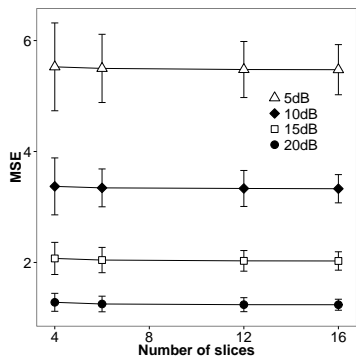
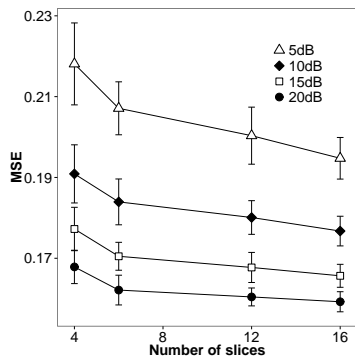
- This maximization is performed using a greedy iterative algorithm which updates the value $u_{i,j,k}$ at each node by using the neighboring values from the previous iteration.
- The iterative scheme can be expressed simply using a linear update:

$$\mathbf{u}^{(new)} = \text{initial condition} + \mathbf{A}\mathbf{u}^{(prev)}.$$

where the matrix \mathbf{A} has only 6 non-zero entries in each row.

- This iterative scheme is guaranteed to converge which can be proved using a contraction mapping argument [Ingle, Varghese, Sethares 2015 (under review)].

Simulated Ellipsoidal Inclusion



- Reconstruction MSE on a simulated ellipsoidal inclusion for different noise levels compared to nearest neighbors interpolation; Markov random field algorithm (left), nearest neighbors (right).

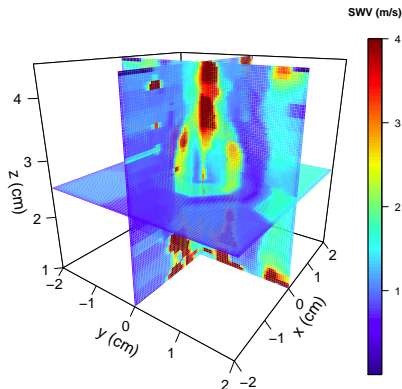
Experimental Results

Signal to noise ratios

ROI	Algorithm	4 slices	6 slices	12 slices	16 slices
bkg	MRF	22.65	23.14	21.72	17.78
	NNB	21.74	21.87	20.24	16.21
inc	MRF	11.14	11.34	10.72	10.47
	NNB	9.03	9.21	8.51	8.22

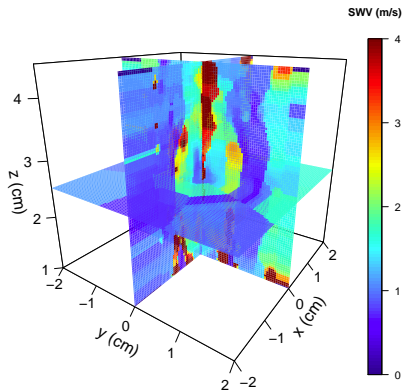
- Signal to noise ratios (SNR) in dB calculated from parallelepiped shaped ROIs in the background and inclusion. The MRF reconstruction has a higher SNR in all cases. (MRF=Markov random field algorithm, NNB=nearest neighbors interpolation, bkg=background, inc=inclusion).

Experimental Results



- **Markov random field reconstruction** appears less blocky and has higher SNR than nearest neighbor interpolation.

Experimental Results



- Markov random field reconstruction appears less blocky and has higher SNR than nearest neighbor interpolation.

Summary

- A sheaf acquisition method that extends 2D imaging methods to 3D was developed.
- The effect of varying number of imaging planes in the sheaf was also analyzed.
- Approximate reconstruction algorithms that generate 3D visualization from a stack of C-planes were developed.
- A fast full-3D reconstruction algorithm that provides better SNR than nearest neighbor interpolation was also presented.

Conclusion

- We demonstrated the use of plane wave imaging and angular compounding for high frame rate tracking in electrode vibration elastography.
- We developed a model-based noise filtering techniques for 2D shear wave velocity reconstruction that provide better MSE performance than standard algorithms for calculating derivative from noisy data.
- We also developed 3D reconstruction algorithms that can be used for visualizing the ablated 3D volume by stitching together data from 2D imaging planes.
- These algorithms were compared against standard techniques used in literature and were shown to provide better image quality metrics such as SNR.
- These algorithms are “general purpose,” in that can be applied to reconstruct strain, stiffness, temperature maps, coherence maps, or even for other signal processing applications outside medical imaging.

List of Publications

● Journals

- A. Ingle, T. Varghese, "Three Dimensional Sheaf of Ultrasound Planes Reconstruction (SOUPR) of Ablated Volumes," IEEE TMI (2014).
- A. Ingle, J. Bucklew, W. Sethares, T. Varghese, "Slope Estimation in Noisy Piecewise Linear Functions," Signal Processing (2015).
- A. Ingle, T. Varghese, "A Kernel Based Inversion Algorithm for 3D Ultrasound Elastography," (under review).
- A. Ingle, T. Varghese, "Ultrasound Based Tracking of Shear Waves using a Particle Filter Denoising Approach," (under review).
- A. Ingle, T. Varghese, W. Sethares, "Efficient 3D Reconstruction in Ultrasound Elastography via a Sparse Iteration based on Markov Random Fields" (under review).

● Conferences

- A Comparison of Model Based and Direct Optimization Based Filtering Algorithms for Shear Wave Velocity Reconstruction in Ultrasound Electrode Vibration Elastography (ISBI 2013)
- C-plane Reconstructions from Sheaf Acquisition for Ultrasound Electrode Vibration Elastography (IEEE UFFC 2014)
- Stochastic Piecewise Linear Function Fitting with Application to Ultrasound Shear Wave Imaging (IEEE EMBC 2014)
- Three Dimensional Shear Wave Elastographic Reconstruction of Ablations (IEEE EMBC 2014)
- Piecewise Linear Slope Estimation (Asilomar 2014)

● Patents Pending

- Rapid Three-Dimensional Elasticity Imaging (US 20140243666A1)
- TOTAL3D: Algorithm for Complete 3D Visualization of Structures in Ultrasound Elastography (WARF: P140237)

Acknowledgments

- NIH-NCI (for the funding support R01CA112192-S103 and R01CA112192-05/6/7).
- Prof. Tomy Varghese for his advice, constant encouragement and trust in my work.
- Prof. William Sethares for the numerous wonderful discussions on a variety of topics.
- Profs. John Gubner, Tim Hall and Chris Brace for serving on my committee.
- Profs. Jim Zagzebski and Jim Bucklew for discussing ideas.
- Prof. Ernie Madsen and Gary Frank for help with phantoms and experiments.
- Ultrasound lab members for delightful camaraderie.
- Numerous friends I have made during my stay in Madison.
- Parents, brother and rest of the family back home for their unconditional love and support.

Thank you!

Questions?